Ultrafast excitation quenching by the oxidized Photosystem II reaction center

Parveen Akhtar[1,2,3], Gábor Sipka[2], Wenhui Han[4], Xingyue Li[4], Guangye Han[4], Jian-Ren Shen[4,5], Győző Garab[2], Howe-Siang Tan[1*], Petar H. Lambrev[2*]

[1] School of Physical and Mathematical Sciences, Nanyang Technological University, Nanyang Link 21, 637371, Singapore

[2] Biological Research Centre, Szeged, Temesvári krt. 62, Szeged 6726, Hungary

[3] ELI-ALPS, ELI-HU Non-profit Ltd., Wolfgang Sandner u. 3, Szeged 6728, Hungary

[4] Photosynthesis Research Center, Key Laboratory of Photobiology, Institute of Botany, Chinese Academy of Sciences, Beijing, China

[5] Research Institute for Interdisciplinary Science, and Graduate School of Natural Science and Technology, Okayama University, Okayama, Japan

[*] Corresponding authors, e-mail: howesiang@ntu.edu.sg, lambrev.petar@brc.hu

ORCID IDs: 0000-0002-3264-7154 (P.A.); 0000-0002-8553-4890 (G.S.); 0000-0003-3373-2008 (G.H.); 0000-0003-4471-8797 (J.-R.S.); 0000-0002-3869-9959 (G.G.); 0000-0003-2523-106X (H.-S.T.); 0000-0001-5147-153X (P.H.L)

ABSTRACT

Photosystem II (PSII) is the pigment-protein complex driving the photoinduced oxidation of water and reduction of plastoquinone in all oxygenic photosynthetic organisms. Excitations in the antenna chlorophylls are photochemically trapped in the reaction center (RC) producing the chlorophyll–pheophytin radical ion pair P^+ $Pheo^-$. When electron donation from water is inhibited, the oxidized RC chlorophyll P^+ acts as an excitation quencher, but knowledge on the kinetics of quenching is limited. Here we used femtosecond transient absorption spectroscopy to compare the excitation dynamics of PSII with neutral and oxidized RC (P^+). We find that equilibration in the core antenna has a major lifetime of about 300 fs, irrespective of the RC redox state. Two-dimensional electronic spectroscopy revealed additional slower energy equilibration occurring on timescales of 3–5 ps, concurrent with excitation trapping. The kinetics of PSII with open RC can be described well with previously proposed models according to which the radical pair P^+ $Pheo^-$ is populated with a main lifetime of about 40 ps that is primarily determined by energy transfer between the core antenna and the RC chlorophylls. Yet, in PSII with oxidized RC (P^+), fast excitation quenching was observed with decay lifetimes as short as 3 ps and an average decay lifetime of about 90 ps that is shorter than the excited-state lifetime of PSII with open RC. The underlying mechanism of this extremely fast quenching prompts further investigation.

INTRODUCTION

Photosystem II (PSII) is the only biological system capable of catalyzing the photooxidation of water in plants, algae and cyanobacteria, releasing oxygen in the atmosphere as a by-product [1]. Structurally and functionally the PSII core complex can be divided into reaction center (RC), containing the electron-transfer chain cofactors (Figure 1) coordinated by the D1 and D2 proteins, core antenna (the CP43 and CP47 chlorophyll-protein complexes) and oxygen-evolving complex (OEC). In most eukaryotic algae and plants the absorption cross-section of PSII is augmented by membrane-intrinsic light-harvesting complexes [2, 3], whereas in cyanobacteria this function is performed by the phycobilisomes [4]. The primary photochemical reaction is the oxidation of one of the RC Chlorophylls (Chl), most likely Chl_{D1}, and reduction of pheophytin $Pheo_{D1}$ [5]. Subsequent ultrafast electron transfer localizes the positive charge on Chl P_{D1} and this is followed by stabilization of the charge-separated state by electron transfer to the primary quinone acceptor Q_A, forming the stable radical pair $P_{D1}^{+}Q_A^{-}$ on a timescale of about 200 ps [6, 7]. The radical cation $P_{D1}^{\bullet +}$ ($P_{680}^{\bullet +}$) is a strong oxidant and is normally reduced by Tyr_Z (Y_Z) on the D1 protein on a timescale of 30–60 ns recovering the neutral ground state of the RC chlorins [8, 9]. These reactions ensure that the concentration of oxidized RC Chls, P^+ (we will use P to denote any RC Chl) in normal physiological conditions under low excitation flux is negligible. However, the situation can be different under high light conditions, especially when combined with other environmental stress factors, when the normal photosynthetic electron-transport chain is overwhelmed.

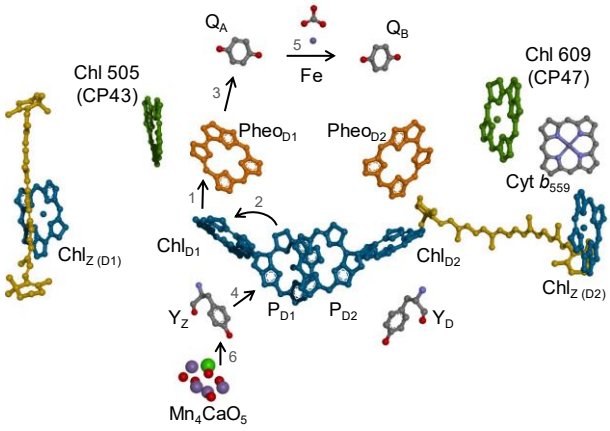

Figure 1. Schematic arrangement of the cofactors in the PSII RC and the main electron-transfer pathway from the primary electron donor (Chl_{D1} or P_{D1}) to the terminal quinone acceptor (Q_B) and from the water-oxidizing Mn_4CaO_5 cluster to P_{D1}. The numbers indicate the sequence of events, based on the relative reaction rate constants. The location of the nearest-neighbor antenna Chls is also shown (in green) for reference. The figure is created in Biovia Discovery Studio using PDB 3WU2 [10]. Adapted from [11].

In PSII with active, open RC, excitations in the antenna are trapped with an apparent lifetime of 30–60 ps [12-15], which accumulates the charge-separated state P^+ $Pheo^-$. The process evidently involves several steps – excitation energy transfer (EET) in the antenna and from the antenna to the RC and one or more electron-transfer steps. For decades the validity of two opposing kinetic models has been

debated – the trap-limited model, i.e. charge separation (CS) is the rate-limiting process [13, 16] and the transfer-limited model, i.e. the rate-limiting process is EET to the RC [15, 17, 18]. Both models are based on a large number of experimental and theoretical studies, but unequivocal evidence is very hard to obtain, partly because the antenna and RC Chls are almost spectrally indistinguishable. EET in isolated CP43 and CP47 occurs primarily on a subpicosecond timescale [19]. However, longer equilibration components (10–20 ps) are observed under high excitation conditions promoting singlet-singlet annihilation [20]. Transient spectroscopies in the visible and infrared region have identified the rise time of the P^+ $Pheo^-$ radical pair to be a few tens of ps [16, 17, 21, 22] but this in itself does not reveal the contribution of the EET rate to the total trapping time. Structure-based theoretical computations predict slow EET (20–50 ps) from CP43 and CP47 to the RC mainly due to the large distances between the core antenna and RC Chls [23-25]. Polarization-resolved visible/infrared transient absorption spectroscopy (TAS) of PSII crystals has provided evidence for slow (tens of ps) equilibration between CP43 and CP47 across the RC, supporting the transfer-limited model [26].

All oxygenic photosynthetic organisms have evolved mechanisms to sense conditions of excess excitation light and to protect PSII from photodamage and photoinhibition [27]. Non-photochemical quenching (NPQ) of Chl fluorescence is a crucial photoprotective mechanism that accelerates the thermal dissipation of singlet excited states in the PSII antenna Chls [28-31]. The quenching of singlet excitations reduces the probability to generate potentially dangerous Chl triplet states, either directly by intersystem crossing: $^1Chl^* \rightarrow {}^3Chl^*$), or by radical pair recombination: $^1[P^+\ Pheo^-] \rightarrow {}^3[P^+\ Pheo^-] \rightarrow {}^3P^*\ Pheo$ [32]. The main site of NPQ is the peripheral PSII antenna [33-35] but quenching by the RC is also possible [36, 37], especially when the OEC is inactivated [38]. Krieger et al. [39] proposed a RC quenching model wherein in the absence of fast electron donation by the OEC, energy is lost via recombination between P^+ and Q_A^-. An alternative mechanism is direct quenching by P^+. Chl radical cations are known to be potent quenchers of Chl excited states [40]. In other photosynthetic RCs – the purple bacterial RC and Photosystem I (PSI), excitation quenching by the oxidized RC Chls is easily demonstrated and measured. Curiously, in both the purple bacterial RC and PSI, the rate of nonphotochemical excitation quenching by P^+ is almost identical to the rate of photochemical trapping by the neutral RC [41-43]. Bruce et al. [44] observed that the quenching in PSII at low pH, when the OEC is inactivated, was associated with the increased lifetime of P^+ but the fluorescence recovered in the microsecond region whereas $P^+\ Q_A^-$ recombination occurs in the millisecond time range. They concluded that direct excitation quenching by P^+ is the main reason for the decreased fluorescence yield in PSII at low pH. It should be noted that although the radical cation is often denoted P_{680}^+, the positive charge could also reside on Chls other than P_{D1}, particularly Chl_Z [45].

The dynamic properties of PSII with an oxidized RC Chl can be relevant to a range of physiological conditions, as OEC is a fragile component of PSII susceptible to inactivation by high and low temperature, UV radiation and other stress factors [46-48]. Shinkarev and Govindjee [49] modelled the

fluorescence yield of PSII specifically including quenching by P^+, assuming that the rate of quenching is three times slower than the photochemical trapping. The first experimental evidence of the efficiency of quenching was given by Steffen et al. [50], who found that the re-reduction of P^+ observed in a few hundreds of microseconds following a saturating pulse is associated with an increase of the fluorescence yield. It was therefore asserted that P^+ is a more efficient quencher than the open RC. In a more recent time-resolved fluorescence study, Paschenko et al. [51] used saturating laser pulses to induce full oxidation of the RC and probed the fluorescence decay kinetics induced by excitation pulses delayed by several nanoseconds. They found that the fluorescence lifetimes of PSII core complexes or PSII-enriched membranes were shorter when the RCs were preoxidized compared to the lifetimes of the dark-adapted open RCs, confirming that the rate of nonphotochemical quenching by P^+ is higher than the rate of photochemical trapping.

In this study, we used femtosecond transient absorption spectroscopy to compare the excitation dynamics of the isolated PSII core complex of *Thermosynechococcus* (*T.*) *vulcanus* at room temperature under three conditions: in a dark-adapted state with open RCs (Q_A oxidized), closed RCs (Q_A reduced) and closed RCs with preoxidized RC Chls (P^+ Q_A^-). Note that we refer to the former two states as possessing a neutral RC (Chl), as opposed to oxidized RC (Chl), as in the latter. We also employed two-dimensional electronic spectroscopy (2DES) under conditions of open and closed RC, to gain more information on the excitation energy equilibration dynamics as a function of excitation wavelength. The experimental data shows predominantly subpicosecond EET kinetics within the PSII antenna, which is independent of the redox state of the RC, and distinct multiphasic trapping kinetics by the neutral and the oxidized RC on picoseconds-to-nanoseconds timescale.

MATERIALS AND METHODS

Sample preparation and handling

The thermophilic cyanobacterium *T. vulcanus* was grown photoautotrophically as a batch culture in BG11 medium (pH 7) at 323 K under continuous illumination with a white fluorescent lamp at intensity of 50–100 μmol photons m^{-2} s^{-1} photon flux density [52]. PSII core complexes (hereafter called PSII) were isolated from *T. vulcanus* as described earlier [53, 54]. The isolated PSII was diluted in a buffer medium containing 5% glycerol, 20 mM MES (pH 6.0), 20 mM NaCl, 3 mM $CaCl_2$.

For spectroscopic measurements the PSII samples were diluted to absorbance of 0.35 at the Chl *a* Q_y maximum in a 1 mm path length. To keep the RC in an open state the buffer was supplemented with 25 μM dichlophenolindophenol and 0.5 mM ferricyanide, and continuously circulated during the measurement (at a flow rate of 2–4 mL/min), ensuring that the excitation pulses encounter the same PSII complex only once. Measurements with closed RCs were performed by adding 20 μM DCMU to the

buffer medium and either circulating the sample at a lower flow rate or using an additional background illumination source.

Laser spectroscopy setup

Femtosecond TAS and 2DES were performed using the same laser setup described elsewhere [55].

Briefly, the fundamental laser beam centered at 800 nm with 140-fs pulse duration and 1 kHz repetition rate obtained from a commercial regenerative amplifier system (Legend, Coherent) was used to pump a commercial noncollinear optical parametric amplifier (TOPAS, Light Conversion) producing ~30-fs pulses centered at 680 nm with a 50-nm bandwidth (FWHM), that cover the Q_y absorption band of PSII (Supplementary Fig. S1). The TOPAS output was passed through an acousto-optic programmable dispersive filter (AOPDF) pulse shaper unit (Dazzler, Fastlite), to remove the chirp and compress the pulses to nearly transform-limited pulses which are used as excitation pulses. White-light continuum generated by a 2-mm sapphire window was used as a probe beam after compressing with a pair of chirped mirrors. The compressed probe was directed through a mechanical translation stage providing a delay against the pump pulses waiting time (T_w). The polarization of the probe pulse was set to 54.7° (magic angle) with respect to the polarization of the excitation pulses using a half-wave plate and a polarizer. Finally, the pump and probe beams were spatially overlapped on the sample unit and the probe beam was frequency resolved and detected using a spectrometer (TRIAX 190, Horiba) assembled with a CCD (PIXIS 100, Princeton Instruments). The cross-correlation width of the excitation and probe pulses was ~40 fs (FWHM), determined by measuring the optical Kerr effect. Part of the white light was used as a reference beam, using a beam splitter, to correct for intensity fluctuations during the measurements. The T_w delay between the excitation and probe pulses was scanned from −0.1 to 700 ps in a quasilogarithmic progression. To avoid exciton annihilation and the build-up of photoproducts, the experiments were done with excitation pulses of very low energy – 1 nJ, corresponding to approx. 4×10^{13} photons/cm^2/pulse (focused spot diameter of ~100 μm). The maximal transient absorption signal was 2–3 mOD.

TAS measurements of the kinetics of PSII with preoxidized RC (P^+) were performed with additional saturating pulses. To this end, a beam splitter was added at the TOPAS output, thus splitting the beam into “pre-pump” and “pump” paths. The “pre-pump” beam was overlapped with the pump and the probe beams on the same spot on the sample adjusting its optical path so that the “pre-pump” pulses hit the sample ~3 ns before the pump pulses. The “pre-pump” pulse energy was 1 μJ (~5×10^{15} photons/cm^2/pulse, spot size 0.3 mm), which was determined to exert a saturating effect on the P oxidation.

Fourier-transform femtosecond 2DES was performed in a partially collinear “pump-probe” geometry setup (laser setup as described above) producing absorptive 2D spectra. The pulse shaper was programmed to create pulse pairs with controllable inter-pulse delay time and phase difference. The

time delay τ between the two excitation pulses (coherence time) was scanned between 0–150 fs with a 3-fs step. The 2D photon echo signals were recorded by utilizing a 2-phase cycling scheme (φ = 0, 180°) in a partially rotating frame of reference [56]. The signals (2D interferograms) were Fourier-transformed along τ to obtain 2D electronic spectra in the frequency/wavelength domain (with excitation/detection wavelengths λ_τ/λ_t).

RESULTS

Transient absorption spectroscopy of PSII with open and closed RC

We will first compare the broadband TAS data of PSII core complexes with open (dark-adapted state) and closed RCs (in the presence of DCMU), wherein the RC Chls are in their neutral electronic ground state before the pump pulses. Transient absorption spectra at selected delay times are plotted in Supplementary Fig. S2. Global five-exponential decay fitting was applied to the TAS data from 100 fs to 700 ps. The resulting lifetimes and decay-associated absorption difference spectra (DADS) are shown in Figure 2. Evolution-associated difference spectra (EADS), corresponding to the component spectra in a sequential irreversible kinetic model, are plotted in Supplementary Fig. S3. The absorption changes in the wavelength region 610–730 nm reflect ground-state bleaching (GSB), stimulated emission (SE) and induced absorption (IA) of Chl excited states as well as radical ions created after CS. The electric fields generated in the RC after charge separation further induce electrochromic band shifts (Stark effect) on the neighboring pigments [57, 58].

The TAS results of PSII with open RC are similar to the results reported in [16] obtained with 663 nm excitation. Nevertheless, we describe the main relevant features. The initial DADS represents fast processes (0.3–0.4 ps lifetime) of exciton energy equilibration in the core antenna – the approximately conservative spectrum carries signatures of EET from ~670 nm (predominantly in CP43) to ~680 nm. The second kinetic component with lifetime of 4–5 ps can be related to 6–8 ps decay components in Ref. [16]. The DADS shows mainly decay of bleaching around 680 nm but also a shoulder on the blue side and positive amplitude around 690 nm that could be interpreted as EET to the red-shifted Chls in CP47. However, the spectrum is strongly non-conservative (mostly negative), hinting that excitation trapping also occurs on this timescale.

The 40-ps kinetic component is characterized by the decay of the negative SE signals and rise of IA at wavelengths > 700 nm (note that both processes add to the negative DADS amplitude). This is the main trapping lifetime, reflecting the conversion of Chl excited states to the P^+ $Pheo^-$ radical pair [13]. The DADS has a negative peak at 685 nm, a local maximum at 678 nm and a broader negative feature at 670 nm. There can be different possible assignments of these features but phenomenologically the spectrum is characteristic for the charge separation process.

The ~240 ps lifetime shows the subsequent electron transfer from $Pheo^-$ to Q_A [6, 7]. Q_A does not contribute to the absorption in this region but the reduced semiquinone anion can induce electrochromic band shifts of its nearest pigments, primarily $Pheo_{D1}$ [57, 59]. The negative charge on $Pheo_{D1}^-$ in turn induces electrochromic blue shift of the absorption of Chl_{D1} [60]. The sharp negative peak at 683 nm in the 240-ps DADS is primarily a result of the decaying $Pheo_{D1}^-$ and associated loss of bleaching and electrochromic shift (of Chl_{D1}). The final component (the lifetime was fixed to 10 ns) reflects the RC state after the reoxidation of $Pheo_{D1}$ by Q_A: it shows the remaining P bleaching, P^+ absorption and electrochromic shifts (of Chl_{D1} and $Pheo_{D1}$).

In PSII with closed RC the first two DADS, lifetimes of 0.34 ps and 3.6 ps (Figure 2A), are rather similar to that of PSII with open RC (Figure 2B). This is due to the fact that both exhibit no dependence on the redox state of Q_A^-, which signals that they originate primarily in the antenna. In PSII with closed RC, charge separation is still possible, but the terminal electron acceptor is Pheo since electron transfer to Q_A is blocked. The 55-ps DADS bears the characteristic features of the 40-ps DADS in open RC and thus can be assigned to the formation of the $P^+ Pheo^-$ state (the DADS are directly compared in Supplementary Fig. S4). In the absence of forward electron transfer, the radical pair $P^+ Pheo^-$ decays via radiative or nonradiative recombination, displaying multiexponential kinetics attributed to protein relaxation [61]. The main decay lifetime of ~2 ns is well documented [44, 61, 62], but shorter decay components are discernible. Note that although the lifetimes can be comparable to those in open RCs, the DADS have distinct shapes (e.g. the 216-ps DADS in closed RC and 239-ps DADS in open RC), as they reflect different processes and intermediates. Also of note is the difference in the ns-component DADS between open and closed RCs. In open RCs the spectrum has a characteristic shape carrying the differential absorbance of $[P^+ Q_A^-]/[P\ Q]$, whereas in closed RC, the absorbance changes reflect $[P^+ Pheo^-]/[P\ Pheo]$. This DADS alone is a qualitative signature of the RC state prior to the pump pulse.

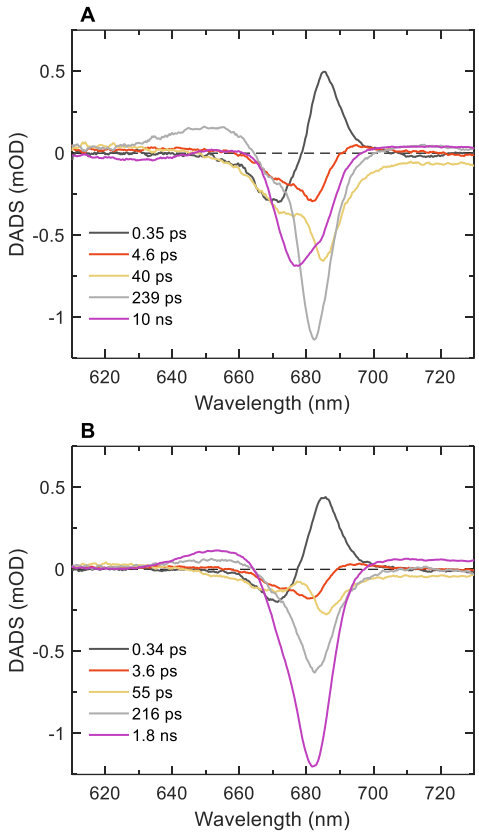

Figure 2. DADS obtained by five-component global lifetime analysis of the transient absorption traces. A: PSII with open RC; B: PSII with closed RC.

Two-dimensional electronic spectroscopy

For more detail into the kinetics of PSII, we compared the excitation wavelength dependence of the spectral evolution with open and closed RC by 2DES, under the same conditions as TAS. In the purely absorptive 2D electronic spectra, the horizontal axis (λ_t) is equivalent to the detection wavelength axis in TAS and the vertical axis (λ_τ) reports the excitation dependence of the absorption changes. Both types of measurements were done with the same excitation (pump) pulses, eliciting the same kinetics in PSII. Global analysis of the transient absorption signal measured during the 2DES experiments as well as of the 2D signal integrated over the excitation wavelength (λ_τ) yielded lifetimes and DADS that were virtually identical to those obtained from TAS (Supplementary Fig. S5).

Selected 2D electronic spectra of dark-adapted PSII core complexes are shown in Supplementary Fig. S6. Note that the 2D electronic spectra are plotted here in increasing wavelength (decreasing frequency) scale, for the sake of easier comparison with the (one-dimensional) transient absorption spectra. Global five-component analysis of the 2DES data yielded similar lifetimes (0.35 ps, 4 ps, 40 ps, 200 ps and >5 ns). The 2D decay-associated spectra (2D DAS) of the first two kinetic components (Figure 3) clearly indicate exciton equilibration, which produces symmetric negative-positive peak pairs below and above the diagonal, representing downhill and uphill EET [63]. The first 2D DAS (0.35 ps), shows a negative diagonal peak at 670 nm and a corresponding positive cross-peak around 672→685 nm ($\lambda_\tau \rightarrow \lambda_t$),

showing EET from higher- to lower-energy states. The reverse EET is represented by the negative diagonal peak at 685 nm and corresponding positive peak at 685→672 nm. At shorter excitation wavelengths (λ_τ < 670 nm), the negative maximum is not on the diagonal but around 670 nm. The spectral shift is evidence of ultrafast energy equilibration processes that are not resolved in the present analysis but have been shown in a 2DES study of PSII core complexes at cryogenic temperatures [64].

The second 2D DAS (4 ps) confirms beyond doubt that energy equilibration continues on this timescale; this is as evidenced by the symmetric downhill and uphill cross-peaks. The peak positions show that the states whose population decays/rises are different compared to the sub-ps equilibration component. The 2D DAS also reveals that the total decay amplitudes (integrated negative amplitudes) outweigh the corresponding rise amplitudes by a factor of 20:1. In contrast, the total positive and negative amplitudes of the first 2D DAS are equal. To better examine the excitation dependence of the two fast kinetic components, we compared the DADS obtained independently from horizontal slices of the 2D spectra at different excitation wavelengths (Supplementary Fig. S7). At all excitations, the second DADS (3–5 ps lifetime) has largely negative amplitudes, strongly suggesting that excitation trapping is the dominant process on this timescale (see discussion below).

No excitation dependence is discernible in the 2D DAS of the longer-lifetime components (37 ps, also see Supplementary Fig. S6), demonstrating that the system has reached excitonic equilibrium. The 2D DAS of PSII with closed RC share the same qualitative features (Supplementary Fig. S8) – energy transfer between shorter- and longer-wavelength Chls is predominantly observed with a 0.4 ps component and to a lesser extent with a 3-ps lifetime, whereas components with lifetimes 40 ps and longer reflect trapping of the equilibrated excitations.

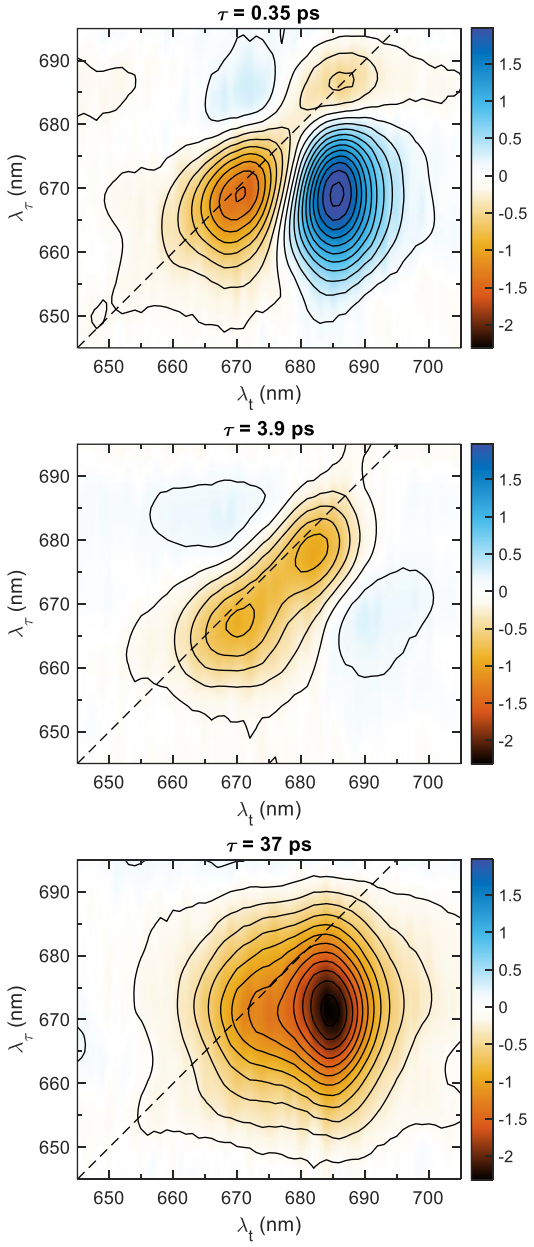

Figure 3. 2D DAS from five-component global lifetime analysis of the 2DES data of PSII with open RC. The contour lines mark 0.2 steps. Red/blue colors represent negative/positive amplitudes (decay/rise of the negative absorptive signal). Only the first three components are shown. The spectra of two long-lived components are omitted as they show no further dependence on excitation wavelength.

Kinetics of PSII with oxidized RC Chls

To probe the kinetics of PSII with a pre-oxidized RC, P^+, we applied two pump pulses separated by a delay of approximately 3 ns. In dark-adapted PSII, the first pulse, which had saturating intensity, creates the stable charge-separated state $P^+Q_A^-$ decaying in tens of nanoseconds. Thus, the second pump pulse finds the RC in a closed state with a Chl radical cation that is expected to quench excitations nonphotochemically. The kinetic traces at 670 nm and 683 nm (Figure 4) show that excitation decay in this case is indeed significantly faster than in either open-state or closed-state RC. It is evident that the

quenching spans different timescales – from a few ps extending to hundreds of ps. Within 5 ps the bleaching signal at 675 nm decayed by 40% (Figure 4A) and at 684 nm – by 20% (Figure 4C). In contrast, the signal decay in PSII with either open or closed RC was 20% and 5–7%, respectively. These results show that quenching by P^+ is substantially faster than photochemical trapping.

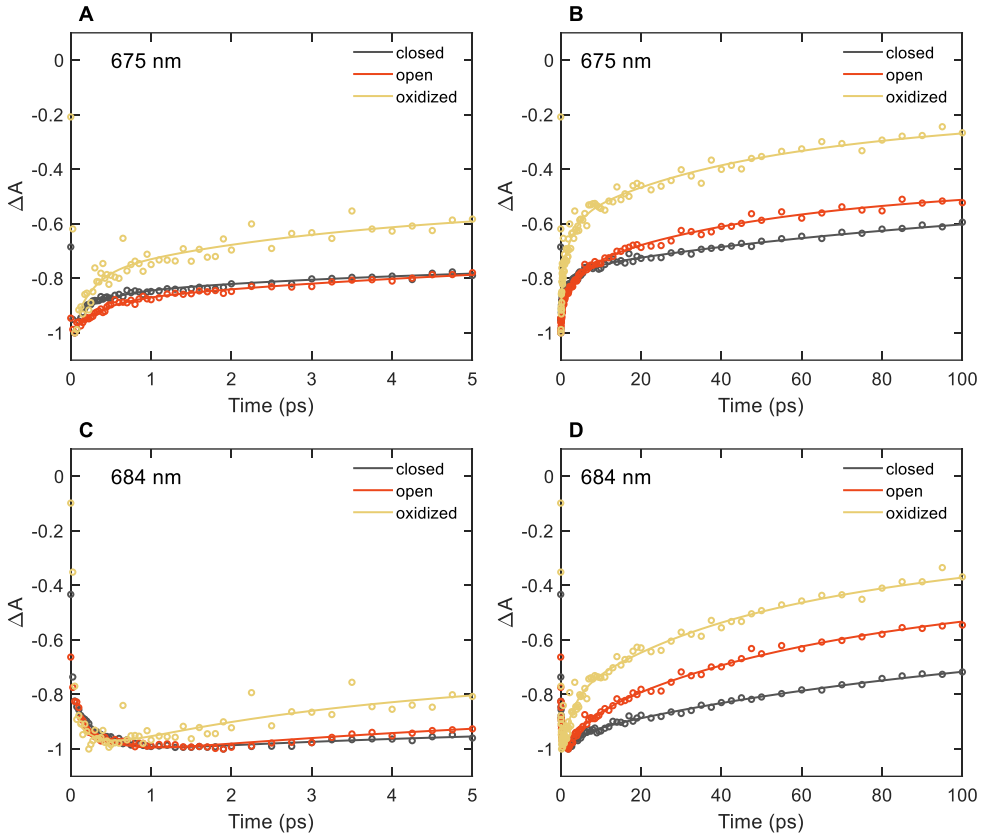

Figure 4. Kinetic traces of the transient absorption of PSII with closed, open, or oxidized RC. A, B: transient absorption at 675 nm; C, D: transient absorption at 684 nm. The symbols show the measured data points and the solid lines are fitted curves obtained by global analysis of the kinetics. The traces are normalized to the maximal negative amplitude.

Global lifetime analysis of the TAS data resulted in four decay lifetimes – 0.24, 2.8, 33, and 180 ps plus a non-decaying component (Figure 5). The fastest lifetime represents energy equilibration in the antenna, as in dark-adapted open RC. However, all other lifetime components (3–180 ps) are negatively-valued and thus reflect only excitation decay, or quenching (Figure 5A). The DADS are qualitatively different compared to the DADS of PSII with open or closed RCs (Supplementary Fig. S4), lacking the features characteristic for the charge-separated states. None of the DADS or EADS resemble the P^+ $Pheo^-$ state, which is formed in either open or closed RCs.

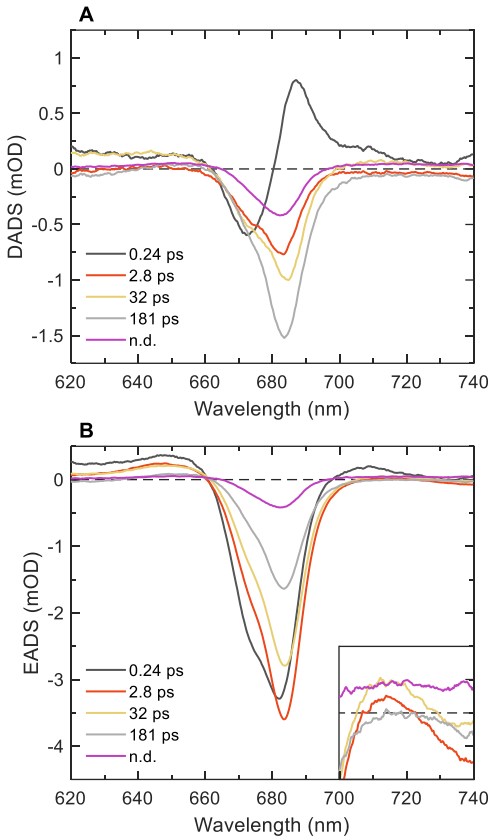

Figure 5. Transient absorption spectroscopy of PSII with pre-oxidized RC (P^+). A. DADS obtained by five-exponential global fitting of the transient absorption traces. B. EADS. The spectra in the region 700–740 nm are magnified (10×) in the inset.

The decay components with lifetimes of 2.8, 32 and 181 ps have relative amplitudes a_r = 23, 31, and 46%, respectively, at 683 nm, resulting in an average decay lifetime $\tau_{av} = 94$ ps ($\tau_{av} = \sum \tau \cdot a_r$). By comparison, the average decay lifetimes calculated from the data shown in Figure 2 for open and closed RCs (excluding the 10-ns component) were ~130 ps and ~1 ns, respectively. These values are similar to the measured average fluorescence lifetimes of PSII from *T. vulcanus* [62]. We can thus estimate that the rate of excitation quenching by P^+ is on average ~40% faster than the photochemical trapping, in line with the fluorescence measurements reported by Paschenko et al. [51].

Interestingly, the spectrum of the non-decaying component (Figure 5B) hints that a stable radical ion pair can be generated, at least in a fraction of RCs, even if P^+ is already present. The spectrum is assigned to a Chl radical because of the characteristic IA in the far-red region (see inset on Figure 5B) – in contrast, the EADS of the decaying lifetime components show distinctive SE at 740 nm associated with the Chl vibronic wing. We can safely rule out the possibility that the long-lived component represents the $P^+ Q_A^-$ state formed in a fraction of RCs that have not been oxidized by the pre-flash. Not only was the intensity of the pre-pulse chosen to be saturating but the DADS is qualitatively different from the spectrum of the $P^+ Q_A^-$ state observed in measurements on PSII with open RC (Figure 2, Supplementary Fig. S4). Therefore, a radical pair different from $P_{D1}^+ Pheo_{D1}^-$ might be created in RCs which already contain P_{D1}^+. However, the quantum yield of this process is low and it by no means represent the main

route of excitation decay – most excitations are effectively quenched by P^+ before electron transfer can take place.

DISCUSSION

Our time-resolved experiments as well as previous studies on PSII core complexes with open RC have shown that the trapping of antenna excitations spans multiple timescales. There could be several potential explanations for the observed 3–5 ps decay component. One is that the component represents mainly energy equilibration within the antenna, as ascribed by van der Weij-de Witt [15]. The predominantly negative DADS and 2D DAS, however, strongly indicate that the main process is excitation loss (trapping). In principle the non-conservative DADS can reflect not only excitation decay, but also equilibration between coupled pigment pools with different total oscillator strength. These two situations can be distinguished by 2DES (Details found in Supplementary Material) by examination of slices at different excitation wavelengths (Supplementary Fig. S7). Such analysis shows that the non-conservative DADS most likely reflects excitation decay.

Secondly, we can rule out singlet-singlet and singlet-triplet annihilation as decay channels because of the low excitation conditions (0.15 excitations per PSII monomer per pulse) and repetition rate (500 Hz). We estimate ~4% maximum probability for excitation loss via singlet-annihilation occurring over any timescale – significantly less than the amplitude of the 4-ps decay. Moreover, doubling the excitation pulse energy did not increase the decay amplitude (data not shown). Singlet annihilation becomes detectable at much higher excitation rates [65].

In the framework of a trap-limited model, multiple kinetic components result from the coupling of sequentially reversible CS steps [13, 14, 16, 66, 67]. However, the present view is that the PSII kinetics is limited by EET from the core antenna to the RC (in tens of ps), which determines the main apparent trapping time. Within a pure transfer-limited model, where the processes of energy equilibration in the antenna as well as the primary CS are significantly faster, virtually monoexponential dynamics can be expected, which is contrary to the body of experimental evidence. On the other hand, non-exponential decay kinetics, approximated with multiple exponential components, could also be explained with dynamic fluctuations (disorder) in the antenna complexes even with irreversible CS [68, 69]. It must be said though that completely irreversible CS is not plausible – charge recombination in PSII repopulating antenna excited states is well documented and is the basis of routine measurements such as delayed light emission [70].

The rate-limiting process in the kinetics is intuitively illustrated by the relationship $\tau_{tot} = \tau_{EET} + \tau_{CS}$, i.e. the total trapping time is the sum of the EET and CS times [71]. In the trap-limited case $\tau_{CS} > \tau_{EET}$ [as in 16]; conversely, in the transfer-limited case $\tau_{EET} > \tau_{CS}$. An intermediate regime is proposed by van der

Weij-de Witt [15]. The main fluorescence decay time (about 40 ps) is determined primarily by EET to the RC but the effective EET and CS times are of comparable magnitude, despite a very fast intrinsic charge separation (0.5 ps^{-1}). Van der Weij-de Witt et al. assign a 7–8 ps lifetime component to equilibration between blue-shifted and red-shifted Chls within the core antenna complexes. However, our TAS and 2DES results unequivocally show that the antenna equilibration has a major lifetime of ~300 fs, which is consistent with measurements on isolated core antenna complexes [19]. Further, we find that the 4-ps lifetime is associated with detectable excitation decay. Therefore, it is reasonable to include this component in the trapping kinetics. To this end, we tested sequentially reversible schemes similar to the one in van der Weij-de Witt [15] and found that both transfer-limited and trap-limited scenarios can fit the data (Supplementary Fig. S9). In the former case, the aggregate rate constant of energy transfer to the RC is ~25 ns^{-1}, contributing strongly to the 40-ps lifetime, whereas electron transfer within the RC is responsible for the observed 3–4 ps lifetime. The model is similar to the one proposed by Pawlowicz et al. [17] based on midinfrared transient absorption spectroscopy of PSII core complexes and is in reasonable agreement with theoretical calculations [18, 72]. However, we stress that models with faster energy transfer rates [as in 14, 16] result in equally good or better fit.

It is worth analyzing in detail the spectral evolution associated with the trapping time of 40–50 ps. The DADS of either open or closed RC show very similar features, which is not surprising as it is known that primary charge separation and P^+ $Pheo^-$ formation occurs in both cases. The main negative transient absorption signal shows an unmistakable blue shift on this timescale, which confers a negative peak (minimum) at 685 nm and a local maximum at 678 nm to the DADS (Figure 2). As discussed above, the transient spectrum of the P^+ $Pheo^-$ state sums not only the bleaching of P_{D1} and $Pheo_{D1}$ but also absorption of the radical ions and electrochromic shifts of the neighboring pigments (mainly Chl_{D1}) and cannot be decomposed without precise knowledge of the exact positions, intensities and bandwidths of these features. On the other hand, close inspection of the 240-ps EADS component in open RCs and the final 1.8-ns EADS in closed RC reveals that they are identical in shape (Supplementary Fig. S10). This is a strong evidence that both spectra are associated with the same radical pair state, safely assigned to P_{D1}^+ $Pheo_{D1}^-$, which is formed with high quantum yield regardless of the redox state of Q_A.

The most striking result of this study is the very fast nonphotochemical quenching of excited states by the oxidized RC, P^+. To our knowledge, this is the first report of quenching components in the range of 3 ps. The short intense laser pulses can in principle generate different quenching species in both the antenna and RC, apart from the radical cation P^+. Within the 3-ns window after the pre-flash, we need to consider the formation of triplet excited states $^3Chl^*$ and, subsequently, $^3Car^*$, both of which are efficient excitation quenchers [50, 73]. Paschenko et al. [51] could resolve fluorescence decay lifetimes of 80–90 ps (plus longer components of hundreds of ps) and assumed that the experimentally observed quenching is partly due to $^3Car^*$. The main pathway for the formation of triplets is by charge recombination of $^3[P^+ Pheo^-]$ creating $^3Chl^*$ states [74] that rapidly migrate, via triplet-triplet energy

transfer, to Cars in the core antenna [75]. The quantum yield of $^3Chl^*$ in the closed-state PSII can be as high as 20–30% [76-78]. However, in the active RC, charge recombination is outcompeted by forward electron transfer to Q_A. From the timescales of EET to Q_A (200 ps) and recombination of $P^+ Pheo^-$ (2–4 ns), it should be expected that the ^3Car yield is ten-fold lower. The proportionality of ^3Car production and Q_A reduction has been experimentally validated [77]. Therefore, charge recombination cannot produce a sizeable population of $^3Car^*$ in our experiments, wherein the RCs are open before applying the saturating laser pulse.

Triplet states can be generated directly in the antenna via intersystem crossing, albeit with a significantly lower yield φ_T (as the rate constant of intersystem crossing, $k_{isc} \approx 0.1$ ns^{-1} [79], is low compared to the photochemical trapping). Yet, strong enough pulses can produce significant population of triplet states [80-82], resulting in detectable fluorescence quenching [50, 83]. The $^3Car^*$ population (per complex) is given by $\chi_T = \varphi_T N_0 \approx k_{isc}\tau^* N_0$, where N_0 is the number of precursor singlet states created in the complex and τ^* the singlet lifetime. For single excitation, φ_T was found to be around 0.1 in CP47 [82]. Under multiple excitation conditions, singlet-singlet annihilation reduces τ^* and, proportionally, φ_T. For our experimental conditions ($N_0 \approx 10$ at 5×10^{15} photons/cm^2/pulse), the mean annihilation time is in the order of 40 ps [65]. This translates to a rather low $\chi_T \approx 0.04$. Furthermore, the degree of $^3Car^*$ quenching should increase with the intensity of the pre-pump pulse. However, we detected no change in the TAS using pre-pump intensities from 0.25 to 3 μJ (Supplementary Fig. S11). Therefore, significant quenching by antenna triplets is unlikely.

The accumulation of other, longer-lived quenchers [81] can be excluded because the illuminated sample is recycled between pump pulses. Thus, we conclude that the principal quencher is P^+. A crude indicator of the quenching efficiency is the amplitude-weighted average decay lifetime of the transient absorption kinetics – 90 ps. In comparison, the average fluorescence lifetime of dark-adapted PSII core complexes is ~130 ps [62]. Thus, the rate of excitation quenching by P^+ is higher than the rate of photochemical trapping in PSII with open RC, in agreement with previous reports [50, 51]. From the average lifetime, one can calculate the quenching rate as $k_q = 1/\tau - k_d$, where k_d is the rate constant of excitation deactivation in the absence of quenching. Assuming $k_d = 0.5$ ns^{-1}, the rate constants of nonphotochemical quenching by P^+ and photochemical trapping by the open RC would be 10.6 ns^{-1} and 7.2 ns^{-1}, respectively.

The existence of the fast (3 ps) quenching component is surprising. It cannot be ascribed to direct excitations in the RC because its amplitude exceeds the probability to excite the RC chlorins. Therefore, the component must reflect, at least partly, quenching of antenna excitations. Presumably the quenching mechanism involves resonance EET to P^+, creating a short-lived higher-excited state of the Chl radical cation. This implies that EET from the antenna to P^+ is faster than to the neutral RC, which is rather surprising as the spectral overlap is evidently smaller. The situation might be reminiscent of the purple bacterial RC, where EET from the accessory Chls to the oxidized P^+ is several orders of magnitude faster than predicted by standard Förster theory [41]. However, there is no complete analogy between PSII

and the bacterial RC, where the strong excitonic coupling of the special pair of BChls drastically alters the energy landscape of the RC in the neutral as well as the oxidized state. Therefore, theoretical understanding of the observed rapid quenching by P^+ in PSII is presently lacking.

Lastly, the nondecaying component in the kinetics of PSII with oxidized RC points to a different mechanism of quenching by P^+ that has not been hitherto documented, i.e. the transient generation of a secondary radical pair in addition to the preformed $P^+ Q_A^-$. Such a mechanism of quenching was proposed to occur in PSI. Giera et al. [43] postulated that in PSI with oxidized RC, $P700^+$, CS can still occur resulting in a different radical pair, probably implicating the accessory Chls, followed by fast nonradiative recombination. This mechanism is supported by the more recent work by Russo et al. [84] in plant PSI-LHCI. A secondary CS in PSII with closed RC can be viewed as supporting the proposed activation of secondary electron transfer pathways in PSII when Q_A is reduced, possibly involving cofactors on the D_2 branch [61, 85].

In conclusion, the TAS and 2DES results presented here demonstrate that trapping of antenna excited states follows complex dynamics with lifetimes as short as a few picoseconds in PSII complexes with either open active RC or pre-oxidized RC (P^+). We find that P^+ provides an extremely efficient pathway for excitation quenching in PSII that evidently endows great capacity for photoprotection under conditions when water-splitting is inhibited.

SUPPLEMENTARY MATERIAL

See Supplementary Online Material for Supplementary Figures S1–S11.

ACKNOWLEDGEMENTS

This work was supported by grants from the National Research, Development and Innovation Office (grants FK-139067 to P.A.; PD-138498 to G.S. and 2018-1.2.1-NKP-2018-00009 to P.H.L.), Eötvös Loránd Research Network (KÖ-37/2021 to G.G. and SA-76/2021 to P.A.), the Singapore Ministry of Education Academic Research Fund (Tier 1 RG2/19 and Tier 1 RG14/20 to H.-S.T.) and National Key R&D Program of China (2017YFA0503700 and 2020YFA0907600 to G.H.), CAS Project for Young Scientists in Basic Research (YSBR-004 to G.H.), a Strategic Priority Research Program of the Chinese Academy of Sciences (XDA26050402 to G.H.).

Data availability

The data that support the findings of this study are openly available in figshare at https://doi.org/10.6084/m9.figshare.18857546.

REFERENCES

[1] J. Barber, Q. Rev. Biophys. **36**, 71 (2003).
[2] P. Cao, X. Pan, X. Su, Z. Liu, and M. Li, Curr. Opin. Struct. Biol. **63**, 49 (2020).
[3] R. Croce, and H. van Amerongen, Science **369**, eaay2058 (2020).
[4] L. Bar-Eyal, A. Shperberg-Avni, Y. Paltiel, N. Keren, and N. Adir, in *Light Harvesting in Photosynthesis*, edited by R. Croce *et al.* (CRC Press, 2018), pp. 77.
[5] H. Tamura, K. Saito, and H. Ishikita, Proc. Natl. Acad. Sci. U.S.A. **117**, 16373 (2020).
[6] A. M. Nuijs, H. J. van Gorkom, J. J. Plijter, and L. N. Duysens, Biochim. Biophys. Acta **848**, 167 (1986).
[7] G. H. Schatz, H. Brock, and A. R. Holzwarth, Proc. Natl. Acad. Sci. U.S.A. **84**, 8414 (1987).
[8] K. Brettel, E. Schlodder, and H. T. Witt, Biochim. Biophys. Acta **766**, 403 (1984).
[9] H. J. Eckert, and G. Renger, FEBS Lett. **236**, 425 (1988).
[10] Y. Umena, K. Kawakami, J. R. Shen, and N. Kamiya, Nature **473**, 55 (2011).
[11] F. Muh, and A. Zouni, Frontiers in Bioscience-Landmark **16**, 3072 (2011).
[12] G. H. Schatz, H. Brock, and A. R. Holzwarth, Biophys. J. **54**, 397 (1988).
[13] Y. Miloslavina, M. Szczepaniak, M. G. Muller, J. Sander, M. Nowaczyk, M. Rogner, and A. R. Holzwarth, Biochemistry **45**, 2436 (2006).
[14] G. Tumino, A. P. Casazza, E. Engelmann, F. M. Garlaschi, G. Zucchelli, and R. C. Jennings, Biochemistry **47**, 10449 (2008).
[15] C. van der Weij− de Wit, J. Dekker, R. van Grondelle, and I. van Stokkum, J. Phys. Chem. A **115**, 3947 (2011).
[16] A. R. Holzwarth, M. G. Muller, M. Reus, M. Nowaczyk, J. Sander, and M. Rogner, Proc. Natl. Acad. Sci. U.S.A. **103**, 6895 (2006).
[17] N. P. Pawlowicz, M.-L. Groot, I. Van Stokkum, J. Breton, and R. van Grondelle, Biophys. J. **93**, 2732 (2007).
[18] G. Raszewski, and T. Renger, J. Am. Chem. Soc. **130**, 4431 (2008).
[19] A. P. Casazza, M. Szczepaniak, M. G. Muller, G. Zucchelli, and A. R. Holzwarth, Biochim. Biophys. Acta **1797**, 1606 (2010).
[20] M. Di Donato, R. van Grondelle, I. H. M. van Stokkum, and M. L. Groot, J. Phys. Chem. B **111**, 7345 (2007).
[21] E. G. Andrizhiyevskaya, D. Frolov, R. van Grondelle, and J. P. Dekker, Phys. Chem. Chem. Phys. **6**, 4810 (2004).
[22] Y. Yoneda, Y. Nagasawa, Y. Umena, and H. Miyasaka, J. Phys. Chem. Lett. **10**, 3710 (2019).
[23] S. Vasil'ev, P. Orth, A. Zouni, T. G. Owens, and D. Bruce, Proc. Natl. Acad. Sci. U.S.A. **98**, 8602 (2001).
[24] Y. Shibata, S. Nishi, K. Kawakami, J. R. Shen, and T. Renger, J. Am. Chem. Soc. **135**, 6903 (2013).
[25] S.-T. Hsieh, L. Zhang, D.-W. Ye, X. Huang, and Y.-C. Cheng, Faraday Discuss. **216**, 94 (2019).
[26] M. Kaucikas, K. Maghlaoui, J. Barber, T. Renger, and J. J. van Thor, Nat. Commun. **7**, 13977 (2016).
[27] K. K. Niyogi, Annu. Rev. Plant Physiol. Plant Mol. Biol. **50**, 333 (1999).
[28] P. Muller, X.-P. Li, and K. K. Niyogi, Plant Physiol. **125**, 1558 (2001).
[29] P. Horton, A. V. Ruban, and R. G. Walters, Annu. Rev. Plant Physiol. Plant Mol. Biol. **47**, 655 (1996).
[30] A. V. Ruban, Plant Physiol. **170**, 1903 (2016).
[31] A. V. Ruban, FEBS Lett. **592**, 3030 (2018).
[32] I. Vass, and K. Cser, Trends Plant Sci. **14**, 200 (2009).
[33] L. Dall'Osto, S. Cazzaniga, M. Bressan, D. Paleček, K. Židek, K. K. Niyogi, G. R. Fleming, D. Zigmantas, and R. Bassi, Nat. Plants **3**, 17033 (2017).
[34] L. Nicol, W. J. Nawrocki, and R. Croce, Nat. Plants **5**, 1177 (2019).
[35] A. V. Ruban, Plant Physiol. **181**, 383 (2019).
[36] G. Finazzi, G. N. Johnson, L. Dallosto, P. Joliot, F.-A. Wollman, and R. Bassi, Proc. Natl. Acad. Sci. U.S.A. **101**, 12375 (2004).
[37] A. G. Ivanov, P. V. Sane, V. Hurry, G. Öquist, and N. P. Huner, Photosynth. Res. **98**, 565 (2008).

[38] G. N. Johnson, A. W. Rutherford, and A. Krieger, Biochim. Biophys. Acta **1229**, 202 (1995).
[39] A. Krieger, I. Moya, and E. Weis, Biochim. Biophys. Acta **1102**, 167 (1992).
[40] W. L. Butler, Annu. Rev. Plant Physiol. Plant Mol. Biol. **29**, 345 (1978).
[41] X. J. Jordanides, G. D. Scholes, W. A. Shapley, J. R. Reimers, and G. R. Fleming, J. Phys. Chem. B **108**, 1753 (2004).
[42] T. Owens, S. Webb, R. Alberte, L. Mets, and G. Fleming, Biophys. J. **53**, 733 (1988).
[43] W. Giera, V. Ramesh, A. N. Webber, I. van Stokkum, R. van Grondelle, and K. Gibasiewicz, Biochim. Biophys. Acta **1797**, 106 (2010).
[44] D. Bruce, G. Samson, and C. Carpenter, Biochemistry **36**, 749 (1997).
[45] R. H. Schweitzer, and G. W. Brudvig, Biochemistry **36**, 11351 (1997).
[46] N. Bukhov, and P. Mohanty, in *Concepts in Photobiology*, edited by G. S. Singhal *et al.* (Springer, 1999), pp. 617.
[47] E. Tyystjärvi, Coord. Chem. Rev. **252**, 361 (2008).
[48] R. Gupta, Plant Signal. Behav. **15**, 1824721 (2020).
[49] V. Shinkarev, and Govindjee, Proc. Natl. Acad. Sci. U.S.A. **90**, 7466 (1993).
[50] R. Steffen, H.-J. Eckert, A. A. Kelly, P. Dörmann, and G. Renger, Biochemistry **44**, 3123 (2005).
[51] V. Z. Paschenko, A. A. Churin, V. V. Gorokhov, N. P. Grishanova, B. N. Korvatovskii, E. G. Maksimov, and M. D. Mamedov, Photosynth. Res. **130**, 325 (2016).
[52] J. R. Shen, K. Kawakami, and H. Koike, Methods Mol Biol **684**, 41 (2011).
[53] K. Kawakami, and J. R. Shen, Methods Enzymol. **613**, 1 (2018).
[54] J.-R. Shen, and N. Kamiya, Biochemistry **39**, 14739 (2000).
[55] P. J. Nowakowski, M. F. Khyasudeen, and H.-S. Tan, Chem. Phys. **515**, 214 (2018).
[56] Z. Zhang, K. L. Wells, E. W. J. Hyland, and H.-S. Tan, Chem. Phys. Lett. **550**, 156 (2012).
[57] G. H. Schatz, and H. J. van Gorkom, Biochim. Biophys. Acta **810**, 283 (1985).
[58] A. Y. Mulkidjanian, D. A. Cherepanov, M. Haumann, and W. Junge, Biochemistry **35**, 3093 (1996).
[59] N. Cox, J. L. Hughes, R. Steffen, P. J. Smith, A. W. Rutherford, R. J. Pace, and E. Krausz, J. Phys. Chem. B **113**, 12364 (2009).
[60] E. Schlodder, T. Renger, G. Raszewski, W. J. Coleman, P. J. Nixon, R. O. Cohen, and B. A. Diner, Biochemistry **47**, 3143 (2008).
[61] M. Szczepaniak, J. Sander, M. Nowaczyk, M. G. Muller, M. Rogner, and A. R. Holzwarth, Biophys. J. **96**, 621 (2009).
[62] G. Sipka, M. Magyar, A. Mezzetti, P. Akhtar, Q. Zhu, Y. Xiao, G. Han, S. Santabarbara, J.-R. Shen, P. H. Lambrev, and G. Garab, Plant Cell **33**, 1286 (2021).
[63] P. Akhtar, C. Zhang, T. N. Do, G. Garab, P. H. Lambrev, and H.-S. Tan, J. Phys. Chem. Lett. **8**, 257 (2017).
[64] J. Pan, A. Gelzinis, V. Chorošajev, M. Vengris, S. S. Senlik, J.-R. Shen, L. Valkunas, D. Abramavicius, and J. P. Ogilvie, Phys. Chem. Chem. Phys. **19**, 15356 (2017).
[65] Y. Yoneda, T. Katayama, Y. Nagasawa, H. Miyasaka, and Y. Umena, J. Am. Chem. Soc. **138**, 11599 (2016).
[66] K. Broess, G. Trinkunas, C. D. van der Weij-de, J. P. Dekker, A. van Hoek, and H. van Amerongen, Biophys. J. **91**, 3776 (2006).
[67] K. Broess, G. Trinkunas, A. van Hoek, R. Croce, and H. van Amerongen, Biochim. Biophys. Acta **1777**, 404 (2008).
[68] J. Chmeliov, G. Trinkunas, H. van Amerongen, and L. Valkunas, J. Am. Chem. Soc. **136**, 8963 (2014).
[69] J. Chmeliov, G. Trinkunas, H. van Amerongen, and L. Valkunas, Photosynth. Res. **127**, 49 (2016).
[70] V. Goltsev, P. Chernev, I. Zaharieva, P. Lambrev, and R. J. Strasser, Photosynth. Res. **84**, 209 (2005).
[71] H. van Amerongen, and R. Croce, Photosynth. Res. **116**, 251 (2013).
[72] V. I. Novoderezhkin, J. P. Dekker, and R. van Grondelle, Biophys. J. **93**, 1293 (2007).
[73] L. Valkunas, V. Liuolia, and A. Freiberg, Photosynth. Res. **27**, 83 (1991).
[74] I. Vass, Physiol. Plant. **142**, 6 (2011).
[75] S. Santabarbara, A. Agostini, A. P. Casazza, G. Zucchelli, and D. Carbonera, Biochim. Biophys. Acta **1847**, 262 (2015).

[76] J. R. Durrant, L. B. Giorgi, J. Barber, D. R. Klug, and G. Porter, Biochim. Biophys. Acta **1017**, 167 (1990).
[77] H. Kramer, and P. Mathis, Biochim. Biophys. Acta **593**, 319 (1980).
[78] M. L. Groot, E. J. Peterman, P. J. van Kan, I. H. van Stokkum, J. P. Dekker, and R. van Grondelle, Biophys. J. **67**, 318 (1994).
[79] P. Bowers, and G. Porter, Proceedings of the Royal Society of London. Series A. Mathematical and Physical Sciences **296**, 435 (1967).
[80] R. Schödel, K.-D. Irrgang, J. Voigt, and G. Renger, Biophysical ournal **75**, 3143 (1998).
[81] V. Barzda, M. Vengris, L. Valkunas, R. van Grondelle, and H. van Amerongen, Biochemistry **39**, 10468 (2000).
[82] M. Groot, E. Peterman, I. Van Stokkum, J. P. Dekker, and R. van Grondelle, Biophys. J. **68**, 281 (1995).
[83] R. Schödel, K.-D. Irrgang, J. Voigt, and G. Renger, Biophys. J. **76**, 2238 (1999).
[84] M. Russo, V. Petropoulos, E. Molotokaite, G. Cerullo, A. P. Casazza, M. Maiuri, and S. Santabarbara, Photosynth. Res. **144**, 221 (2020).
[85] V. Martínez-Junza, M. Szczepaniak, S. E. Braslavsky, J. Sander, M. Nowaczyk, M. Rögner, and A. R. Holzwarth, Photochem. Photobiol. Sci. **7**, 1337 (2008).